Proceedings of 2008 ASME Summer Heat Transfer Conference
HT2008
August 10-14, 2008, Jacksonville, Florida USA

HT2008-56155

EFFECTS OF SYNGAS ASH PARTICLE SIZE ON DEPOSITION AND EROSION OF A FILM COOLED LEADING EDGE

Ali Rozati, Danesh K. Tafti and Sai Shrinivas Sreedharan
High Performance Computational Fluid-Thermal Sciences and Engineering Lab
Mechanical Engineering Department
Virginia Polytechnic Institute and State University
Blacksburg VA 24061 USA

Abstract

The paper investigates the deposition and erosion caused by Syngas ash particles in a film cooled leading edge region of a representative turbine vane. The carrier phase is predicted using Large Eddy Simulation for three blowing ratios of 0.4, 0.8 and 1.2. Three ash particle sizes of 1, 5, and 10 microns are investigated using Lagrangian dynamics. The 1 micron particles with momentum Stokes number St = 0.03 (based on approach velocity and cylinder diameter), follow the flow streamlines around the leading edge and few particles reach the blade surface. The 10 micron particles, on the other hand with a high momentum Stokes number, St = 3, directly impinge on the surface, with blowing ratio having a minimal effect. The 5 micron particles with St = 0.8, show the largest receptivity to coolant flow and blowing ratio. On a number basis, 85-90% of the 10 micron particles, 40-50% of 5 micron particles and less than 1% of 1 micron particles deposit on the surface. Overall there is a slight decrease in percentage of particles deposited with increase in blowing ratio. On the other hand, the potential for erosive wear is highest in the coolant hole and is mostly attributed to 5 micron particles. It is only at B.R.=1.2 that 10 micron particles contribute to erosive wear in the coolant hole.

Nomenclature

B.R.	Blowing ratio (u_j^*/u_∞^*)
C_D	Drag Coefficient
d	Coolant hole diameter, particle diameter
D	Leading edge diameter
F	Forces acting on particles
h	convective heat transfer coefficient
h_r	radiative heat transfer coefficient
k	Thermal conductivity
l	Coolant pipe length
L_c	length scale
m	mass
Nu	Nusselt number
p	Coolant hole span-wise pitch
P	Pressure
Re	Reynolds number ($u_\infty D/\nu$)
Re_p	Particle Reynolds number ($\lvert u_f-u_p \rvert d_p/\nu$)
St	Stokes number
t	time
T	temperature
U,u	velocity
V	particle impact velocity
x	Particle location
ρ	Density
τ_v	Momentum response time
τ_{conv}	Convective response time
τ_{rad}	Radiative response time
μ	Dynamic viscosity
θ	non-dimensional temperature

Subscripts

f	Fluid or carrier phase
j	Coolant
conv	convection heat transfer
rad	radiative heat transfer
p	Particle
∞	Free Stream

Subscripts

f	Fluid or carrier phase
p	Particle
*	Dimensional quantity

Introduction

A severe operating environment and residual foulants in fuels derived from alternative sources such as coal and biomass, necessitates taking appropriate measures to reduce the detrimental effects of Deposition, Erosion, and Corrosion (DEC) on the gas turbine engine lifespan. In general, particulate matter in the form of dust, sand, and combustion products pose a severe threat to the durability of hot gas path engine components over a prolonged life span of 1000s of operational hours. According to Wenglarz, [1], the particulate

matter transports to the blade surface through various mechanisms: i) inertial impaction, due to the inertia of the particles which is dominant when the particle diameter is more than a few microns; ii) turbulent eddy diffusion, where the particles are drawn into the turbulent eddies and transported to the surface; iii) thermophoresis, where the temperature difference between the cooled surface and hot gases drives the particles with diameters in the submicron range as large as 0.5 micron; iv) Brownian diffusion by random particle impacts with gas molecules for particle diameters in the range of 0.05-0.1 microns. The damage to the blade surface is not only dependent on the impact mechanism of the particles, but also on particle condition upon impact. Particles can be in the solid, molten, or condensed liquid phase. Studies have shown that corrosion most likely takes place when condensed combustion products impact the surface in the presence of film cooling jets [2]. Erosion and deposition are competitive processes where the dominancy of each depends on the fraction of molten particles in gas. This fraction, in turn, is affected by the particle material composition and gas temperature.

Hamed [3] chose sand particle diameter size of 150 micron to represent the dust laden atmosphere in helicopter engines, and 15 micron diameter ash particles to represent fuel combustion products. Trajectory of the particles showed that while the sand particles deflected from the top blade pressure side and impacted on the bottom blade suction side, the ash particles just hit the pressure side of one blade at the initial row. She also showed the surface impact distribution of sand and fly ash on a two stage engine on the pressure and suction side. In a study by Raubenheimer [4] on land based industrial and marine gas turbine filtration, particles in the range of 0.001-1μm were found to be products of combustion (permanent pollutants). Particles in range of 1-1000μm were ingested from the outside (temporary pollutant), such as sand. Smialek [5] studied the deposition and composition of the particles ingested in helicopter engines which operate in the Persian Gulf. Their analysis concluded that the particles found in the cooling passages are in the size range of 1-10μm and of the same material composition of small sand particles. The melting temperature of these deposits was measured at 1135˚C, based on which, the sand is expected to be molten in the external hot gas path and solid in the coolant flow.

A series of experimental studies have been conducted in the University of Cincinnati [6]. In these studies the rate of erosion was measured for various blade and coating materials based on different particle speed and impingement angle. They also measured the restitution coefficient of the particles which measures the amount of kinetic energy lost by the particle during impact. Particle dynamics and trajectory were modeled and simulated numerically. In general, they found that the small sized particles are more affected by the flow field and approached the gas velocity quickly, while the larger particles are affected by the blade passage geometry. These larger particles generally impacted the suction side of the blade surface due to their negative incidence angle. They also observed that the larger particles bounced back and forth between the blades before they passed through the blade passage. Overall erosion increased the blade tip clearance and blade roughness. Deposition in the cooling flow passage and cooling holes on the blade surface and leading edge leads to blockage of the cooling passages and reduced the efficiency of the internal and film cooling of the blade.

The study of Metwally et al. [7] predicted the blade erosion in an automotive gas turbine engine. They observed that the number of impacts was more significant on the pressure side of guide vane, stator, and rotor blades. On the suction side, impacts mostly took place at the leading edge of the blades. They quantified the blade mass erosion rate by 'blade mass removal per unit area of the blade surface per unit mass of the ingested particles'. The results of erosion rate reduced considerably for the coated blade. They also reported the frequency of impact, impact angle and impact velocity, which had almost similar patterns for coated and uncoated blades. The maximum rate of erosion for the rotor blade was observed at the trailing edge area.

Walsh et al. [8] studied the internal blockage of a single array of cooling holes to investigate the effects of pressure ratio (total coupon pressure to atmospheric pressure), sand amount and distribution, number of holes and metal temperature. Increasing the pressure ratio decreased the chance of blockage by increasing the velocity of the particles. Increasing the amount of sand naturally increased the blockage. The most effective parameter was found to be the coupon metal temperature. As the temperature exceeds 1000˚C, particles would be mostly molten and adhere to the surface.

Bons et al. [9] investigated the deposition rate and thickness for ash from different alternative synfuels: coal, petroleum coke, and biomass. Results showed that the same distribution and size of the particle (10-20 microns) results in an order of magnitude larger deposition for coal and petcoke when compared to biomass. The biomass deposit appeared to adhere to the surface while coal and petcoke deposit could be removed from the surface after shutdown of the system. However, this characteristic could be specific to the operating conditions of the conducted tests in the study. For all alternative fuels, evidence of deposit penetration in to the TBC was found. Crosby et al. [10] studied the "Effects of particle size, gas temperature, and metal temperature on high pressure turbine deposition in land based gas turbine from various synfuels". Two synfuels were selected for the tests. To study the effect of particle size, four different particles diameters were selected. The target coupon was thermal barrier coated (TBC). As the particles became larger, the TBC spallation became more significant. Particle deposition rate decreased with decrease of the gas temperature (temperature threshold was 960˚C). As the surface was cooled, the deposition to the TBC increased.

Sundaram and Thole [11] studied the effects of deposition upstream and downstream of the coolant hole. They found that thin deposition downstream of the leading edge endwall

cooling hole augmented the adiabatic effectiveness. They speculated that this enhancement was due to the limited lift off of the coolant jet as a result of the deposits. With increase in height of the deposition, adiabatic effectiveness decreased. Coolant hole blockage and TBC spallation both decreased adiabatic effectiveness. This negative effect increased with increase in number of partially blocked holes or percentage of spallation. Shah and Tafti [12] investigated potential erosion and deposition of particles in an internal turbine blade ribbed duct. The fully developed turbulent duct flow was predicted by LES and the particle dynamics were investigated in a Lagrangian frame work. They presented the impact distribution of the particles, impingement velocity and angle, and fractional energy transfer to the duct surfaces.

From the literature review it is evident that all past studies pertaining to deposition have assumed ad hoc or field observed blockages or deposition patterns. There has been no study investigating the detailed dynamics of deposition formation under representative hydrodynamic and thermal conditions in the leading edge region of a turbine blade with film cooling jets.

Objective

The present study is the first investigation of the complex two-phase dynamics of deposition formation of residual Syngas ash particulate matter in the leading edge region of a simulated vane with film cooling. The study combines high resolution LES calculations ([13]&[14]) for the carrier phase with detailed Lagrangian particle dynamics ([12]). The effect of jet blowing ratio and particle size or particle Stokes number on deposition and erosion is presented for three particle diameters of 1, 5 and 10 microns with three coolant-to-mainstream blowing ratios of 0.4, 0.8 and 1.2.

Problem Definition

Computational Domain, Boundary Conditions and Mathematical Model for Carrier Phase

The physical system and conditions which are simulated are defined in Table 1. In the computational domain, the leading edge of the blade is represented by a semi-cylinder with a flat after body. Coolant is injected into the mainstream through coolant jets with 30˚compound angle injection. Two rows of film cooling holes are located at ±15˚ from the stagnation line. The diameter of the cylindrical leading edge and the free stream velocity are selected as the characteristic length and velocity scales, respectively, to define the free stream Reynolds number of 100,000. The non-dimensional temperature is defined as $(T^*-T^*_j)/(T^*_\infty-T^*_j)$, where T^*_∞ is the free-stream temperature and T^*_j is the coolant jet temperature. The blade surface is assumed adiabatic, thereby only the coolant and mainstream temperature and their interaction affect the surface temperature distribution. A periodic boundary condition is assumed in the span-wise direction which represents adjacent holes in the row. A symmetry boundary condition is applied along the stagnation line. Figure 1 illustrates the computational domain. The grid consists of 72 hybrid structured/unstructured blocks with a total of 3,866,624 computational cells.

Table 1. Flow properties and leading edge-jet geometry

Leading Edge Geometry	
Blade leading edge diameter (D^*) [m]	0.01
Coolant jet diameter (d^*), [m]	6.3×10^{-4}
Span-wise pitch (p^*/d^*)	4
Flow Properties	
Free stream velocity (U^*_∞), [m/s]	118
Free stream temperature (T^*_∞), [K]	1500
Free stream pressure (P^*_∞), [atm]	20
Free stream density (ρ^*_∞), [kg/m^3]	4.7
Coolant temperature (T^*_j), [K]	800
Coolant-to-mainstream density ratio	1.875[1]
Coolant-to-mainstream blowing ratio (U^*_j/U^*_∞)	0.4,0.8,1.2

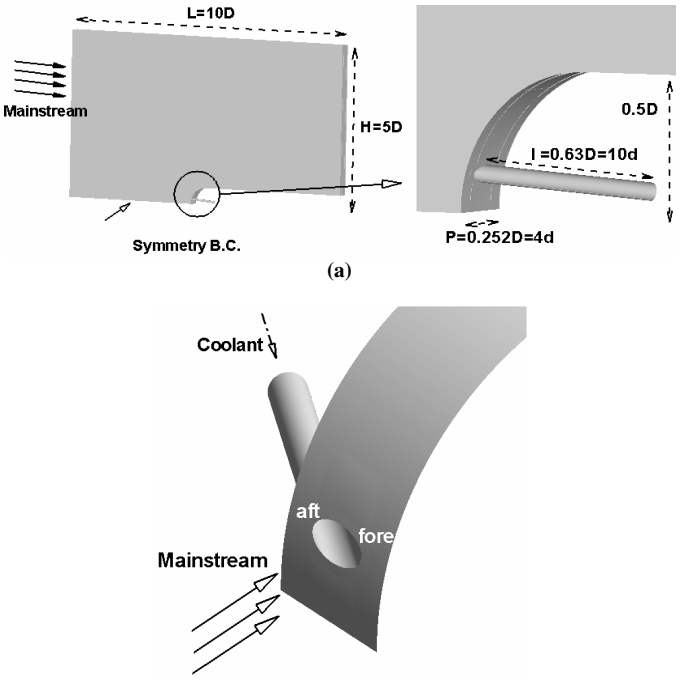

Figure 1. (a) Computational domain; (b) Close-up view of compound angle film cooling jet

The transformed non-dimensional time-dependent incompressible Navier-Stokes and energy equations are solved in a generalized body-fitted coordinate system using Large Eddy Simulations. The turbulent eddy-viscosity is obtained by the dynamic Smagorinsky model. The governing equations of momentum and energy are discretized with a conservative finite volume formulation using a second-order central difference scheme. The temporal advancement is performed with a two-step, semi-implicit predictor-corrector algorithm.

[1] The computations use a ratio of unity.

The adequacy of grid resolution, accuracy of the results, validity of the assumptions and boundary conditions are discussed and established in earlier publications by the authors ([13]&[14]).

Properties, Initial Conditions and Mathematical Model of Dispersed Phase Ash Particles

Properties of Syngas ash vary significantly with coal composition and plant-operating conditions. The common materials in coal ashes are (by wt): 5-70% of Al_2O_3, 0-50% SiO_2, 0-70% Fe_2O_3 0-40% CaO, 0-10% MgO, 0-6% K_2O, 0-10% P_2O_5, 0-10% Na_2O, 0-3% TiO_2 and 0-24% SO_3 [15]. In the current study three ash particle sizes are investigated, 1, 5 and 10 microns with representative density ρ_p=2500 kg/m^3 and specific heat C_p = 250 J/kgK. An important element in ash deposition is its fusibility which is characterized by the initial deformation temperature (IDT), softening temperature (ST), hemispherical temperature (HT), and fluid temperature (FT) [15]. These temperatures vary up to 300-400^{o}C between different ash samples. In the present study a ST of 1100˚K is assumed. It is assumed that ash above this temperature is in a state which facilitates its sticking or depositing on the surface. Any ash particle below this temperature is taken to be in a solid phase and is considered erosive. Erosive ash particles are modeled with elastic collisions with the surface. The velocity and angle of the impact are used to calculate the energy of the impact which could potentially contribute to erosive wear of the surface.

The particle equation of motion is integrated in a Lagrangian frame of reference. The model implementation in an unstructured multiblock multiprocessor framework and validation in turbulent channel flow has been reported in [16]. Application to particulate transport and erosion potential in ribbed internal cooling ducts has been reported in [12,16]. The following equations are used to calculate the particle location and velocity:

$$m_p^* \frac{du_i^{*p}}{dt^*} = \sum F_i^{*p}$$
$$\frac{dx_i^{*p}}{dt^*} = u_i^{*p} \qquad (1)$$

The typical forces acting on the particle are drag, gravitational forces, Saffman lift force caused by the shear of the surrounding fluid, added mass, pressure and viscous forces, Basset forces due to fluid acceleration, Magnus lift force due to particle rotation, and forces due to interparticle collisions. Brownian and thermophoresis forces are also important for submicron sized particles, and are a result of random molecular motion and forces induced by temperature gradients, respectively. For the range of particle sizes investigated in this study (1-10 microns), and for the high density ratio between ash and the carrier phase, the drag force is considered to be the dominant component. Because of the very low concentration of ash (0.02 parts per million by weight (ppmw)), inter-particle collisions and the effect of particles on fluid motion are neglected [12]. Therefore, the simplified equation of particle motion can be written as:

$$\frac{du_i^{*p}}{dt^*} = -\frac{\rho_f^*}{\rho_p^*}\frac{3}{4}\frac{C_D}{d_p^*}\left|u^{*p} - u^{*f}\right|\left(u_i^{*p} - u_i^{*f}\right) \qquad (2)$$

The drag coefficient is given by [17] and is valid for particle Reynolds number up to 700:

$$C_D = \frac{24}{\mathrm{Re}_p}\left(1 + 0.15\,\mathrm{Re}_p^{0.687}\right)$$

Using the free-stream velocity u^*_∞ and the leading edge diameter D^* as the characteristic velocity and length scale, respectively, same as the carrier phase, the particle equations take the non-dimensional form:

$$\frac{du_i^p}{dt} = -\frac{1}{St_p}\left(1 + 0.15\,\mathrm{Re}_p^{0.687}\right)\left(u_i^p - u_i^f\right)$$
$$\frac{dx_i^p}{dt} = u_i^p \qquad (3)$$

where St_p is the particle Stokes number, which is the ratio of the particle time scale τ^*_v to the flow time scale (D^*/u^*_∞),

$$St_p = \frac{\tau_v^*}{D^*/u_\infty^*} = \frac{\rho_p^* d_p^{*2}/18\mu^*}{D^*/u_\infty^*}$$

A large Stokes number indicates that the particle's inertial response to the surrounding fluid is slow, whereas a Stokes number much smaller than unity indicates that the particle closely follows changes in the surrounding carrier phase.

The characteristic equation of particle heat transfer between the two phases is:

$$\frac{dT^{*p}}{dt^*} = \frac{6h^*}{\rho_p^* c_p^* d_p^*}\left(T^{*f} - T^{*p}\right) + \frac{6\varepsilon\sigma}{\rho_p^* c_p^* d_p^*}\left(\left(T_\infty^*\right)^4 - \left(T^{*p}\right)^4\right) \qquad (4)$$

where the first term constitutes the convective heat transfer between the particle and the carrier phase, and the second term constitutes radiative heat transfer which assumes black body radiation between the particle and the surroundings. The convective heat transfer coefficient is obtained from the Ranz and Marshall correlation [18] given by:

$$\frac{h^* d_p^*}{k_f^*} = Nu = 2.0 + 0.6\sqrt{\mathrm{Re}_p}\,\mathrm{Pr}^{1/3}$$

Appropriate non-dimensionalization of equation (4) results in:

$$\frac{d\theta^p}{dt} = \frac{1}{St_{conv}}\left(\theta^f - \theta^p\right) + \frac{1}{St_{rad}}\left(1 - \theta^p\right) \qquad (5)$$

where θ, the non-dimensional temperature is given by (T^*-T^*_j)/(T^*_∞-T^*_j), and the thermal convective and radiative Stokes numbers are given by:

$$St_{conv} = \frac{\tau^{*p}_{conv}}{D^* / u^*_\infty} = \frac{(\rho^*_p c^*_p d^*_p)/6h^*}{D^* / u^*_\infty}$$

$$St_{rad} = \frac{\tau^{*p}_{rad}}{D^* / u^*_\infty} = \frac{(\rho^*_p c^*_p d^*_p)/6h^*_r}{D^* / u^*_\infty}$$

,respectively (h_r^* is the radiative heat transfer coefficient). Similar to the momentum Stokes number, the thermal Stokes numbers represent the thermal inertia of the particle to heat transfer from the carrier phase through convection and radiation.

Table 2 lists the particle Stokes numbers based on the outer flow time scale (D^*/u^*_∞)[2]. At Stokes numbers much less than unity, the particle velocity and temperature respond rapidly to changes in the carrier phase. Based on the values of St_{rad} and equation (5), one can expect that the effect of radiation will be smaller than convection in the energy equation.

Table 2. Particle diameter and Stokes numbers

d_p (micron)	St_p	St_{tconv}	St_{rad}[3]
1	0.029	0.006	1.606
5	0.739	0.154	8.03
10	2.955	0.615	16.06

The particle equations are integrated using a third-order Adams-Bashforth method. A total number of 351,609 particles are injected for each particle size. These particles are uniformly injected at 0.5D upstream of the blade leading edge in a band of p×0.3D, such that their direct line of travel cover the leading edge surface from the stagnation line to 3d downstream of the coolant hole. However, as the particles approach the blade surface, their distribution elongates with the flow in the vicinity of the stagnation line, such that they cover up to 7*d* downstream of the coolant hole. At injection, the particles are in equilibrium with the carrier phase, which is close to the free-stream condition of uniform velocity u_∞ and temperature θ_∞. This is a close approximation to the actual conditions at which the particles would approach the leading edge.

Results

There are two separate mechanisms which affect the deposition and erosion at the leading edge. The first is the interaction of the particles with the outer flow around the cylindrical leading edge and is governed by the outer fluid time scale (D^*/u^*_∞) or the outer Stokes number. The interaction determines whether the particles are transported to the vicinity of the leading edge surface and the coolant jets. The second is the additional interaction of those particles near the surface with the coolant jets, which is determined by d^*/u^*_j and/or the time scale of turbulent eddies.

For particles with large outer Stokes numbers, if the inner time scale is smaller than the outer time scale, the particles exhibit even larger Stokes numbers in the inner region. Hence it is very likely that particles with high Stokes numbers which penetrate to the surface will result in inertial impact unless the jet blowing ratio is high enough to slow the particles enough to avoid impaction. Particles with outer Stokes numbers much less than unity, with little inertia, react to the change in flow path around the leading edge almost instantaneously and follow the flow streamlines, eliminating any contact with the surface. However, in this case, particles traveling close to the surface are receptive to the influence of turbulent eddies generated by coolant jet-mainstream interaction. Between the two extremes is a range of particles which have just enough inertia to penetrate into the inner layer but which are also receptive to turbulent eddies in the inner layer.

Except for particles with large Stokes numbers which are completely driven by inertia, the dynamics of deposition and erosion is strongly influenced by the turbulent structure of the coolant-jet mainstream interaction. A key feature of leading edge film cooling flow which influences the flow field and heat transfer is the entrainment of the hot mainstream gases from the aft-side of the coolant jet. The entrainment, which is due to the formation of a low pressure region immediately downstream of the coolant hole, is shown in Figure 2. To show the three-dimensional nature of entrainment, the time averaged streamlines are imposed on the temperature iso-surface with value of 0.7 (to represent the coolant) at B.R.=1.2. As illustrated, the aft-side vortex structure draws the mainstream flow underneath the coolant. At this blowing ratio the low pressure region is strong enough to create a slight reversed flow, where the mainstream is drawn towards the fore-side and leeward edge of the coolant hole. In spite of being weaker, the dynamics of entrainment at B.R. = 0.4 and 0.8 follows the same general pattern. The entrainment of hot gases also affects the dynamics of deposition and erosion on the surface.

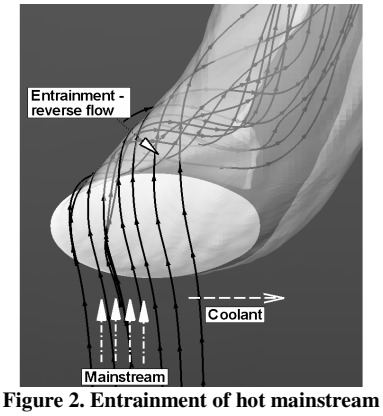

Figure 2. Entrainment of hot mainstream

Deposition

Figure 3 shows the surface distribution of the deposited particles. The contours are indicative of the percentage of injected particles of each size that impact the surface and result in deposition. An immediate observation is the relative

[2] The convective Stokes number is calculated assuming Nu≈2 for Re_p<1.

[3] These are the minimum possible values of radiative Stokes number when $T_p=T_\infty$.

insensitivity of deposition pattern and density of 10 micron particles on the presence of the coolant jet and the blowing ratio. These particles are driven by their free stream momentum and due to their relatively large Stokes number, (both momentum and thermal) they neither react to the flow field nor to the temperature near the leading edge and more than 85% of the injected particles deposit on the surface (Figure 5). Only at BR=1.2, a small distortion in the surface deposition is observed.

For the 1 micron particles, because of the low Stokes number, the particles follow the outer flow streamlines around the leading edge. Particles traveling in the vicinity of the coolant jet-mainstream interaction region are easily entrained and this interaction becomes the driving force for deposition. As the blowing ratio increases and the jet penetrates more into the mainstream, it entrains more particles to the surface, which increases deposition especially at the aft side of the coolant hole as indicated by the entrainment dynamics in Figure 2.

The 5 micron particles are also sensitive to the blowing ratio. With an increase in blowing ratio, the momentum of the coolant succeeds in pushing some particles away from the surface in its direct path; at the same time, entrainment on the aft-side results in more deposition in this region. It is noteworthy that an increase in blowing ratio increases the number of deposited 1 micron particles, but decreases this number for 5 and 10 micron particles.

Deposition in the coolant hole is also dependant on the particle size. 1 micron particles result in no deposition in the hole. Their small momentum Stokes number prevents them from having any contact with the hole surface. Results in Figure 4 shows that the 10 micron particles have the highest rate of deposition on the foreside-downstream wall of the coolant hole, which is in the direct line-of-sight of the oncoming free stream flow. These particles carry their mainstream momentum and enter the coolant hole. Due to their high thermal Stokes number and small residency time within the coolant, they maintain a temperature higher than the ST at impact and mainly result in deposition rather than any erosion (only at BR=1.2 do some of the particles become erosive). The rate of deposition decreases slightly with the increase in blowing ratio. The 5 micron particles result in both deposition and erosion in the hole. Deposition occurs in the same place as for the 10 micron particles, and decreases considerably with an increase in the blowing ratio.

To obtain a overall picture of how the particles react to the main flow and near coolant flow structures, the portion of deposited particles (%numbers) is shown in Figure 5. The data shows that approximately 90% of 10 micron and 41-47% of the 5 micron particles deposit on the surface. Increase in blowing ratio increases the number of deposited 1 micron particles by nearly two orders of magnitude. Results also show that unlike 1 micron particles, 5 and 10 micron particles have slightly less number of particles depositing as blowing ratio increases, due to a stronger coolant jet which forces them away from the surface.

Erosion

In this study, particles with temperatures less than the threshold ST value are assumed to be in a solid state and erode the surface at impingement. Erosion at the surface depends on a number of factors including material characteristics of the surface and particle, impingement velocity, and impingement angle. Characterizing the actual erosion is outside the scope of this paper. Here, the number of particles impacting the surface at a given location, the impact velocity, and impact angle are used to estimate the potential erosive wear by calculating the fraction of incoming particle energy impacting the surface; assuming that on impact all the particle energy is imparted to the surface.

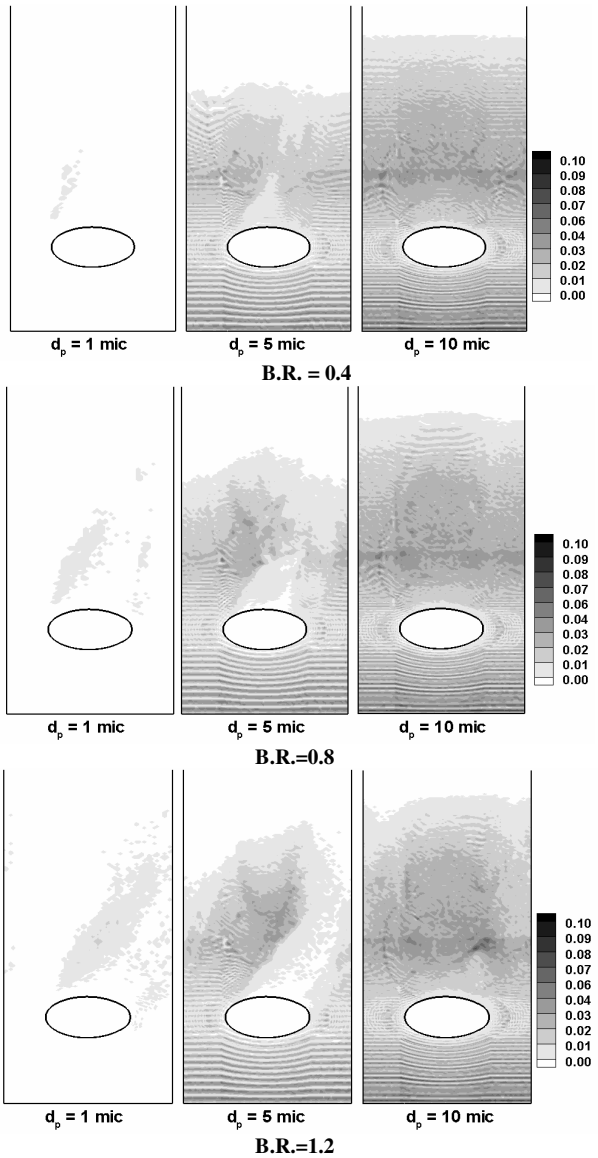

Figure 3. Distribution of %deposited particles of each particle size on the surface

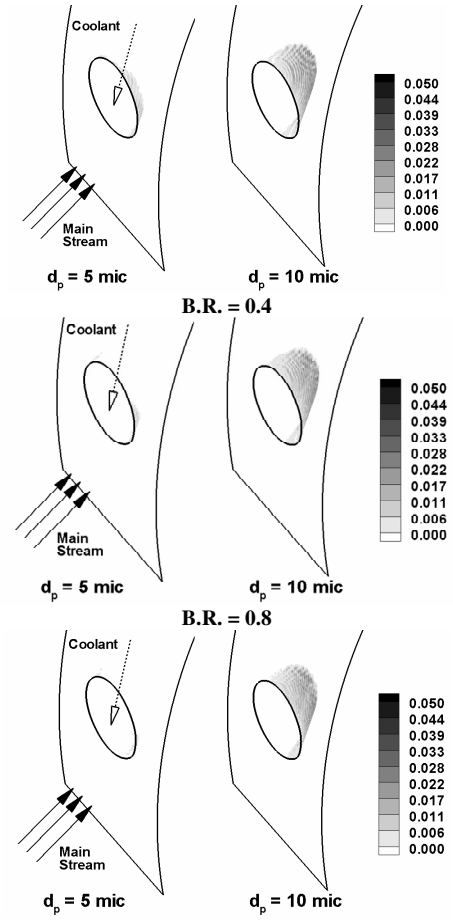

Figure 4. Distribution of %deposited particle of each particle size in the coolant hole

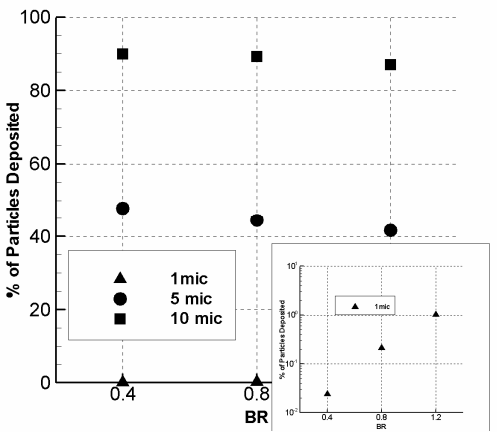

Figure 5. Percentage of deposited particles of each size.

Out of the investigated particle sizes, only the 5 micron particles are found to be erosive on the surface. Both 1 and 10 micron particles only result in deposition on the blade surface as shown earlier. Figure 6 shows the surface distribution of 5 micron erosive particles. The contour shows the percentage of erosive particles out of the total number of 5 micron particles in the flow field. The increase of blowing ratio decreases the number of erosive particles by two means: i) a stronger coolant jet pushes the particles away from the surface and ii) particles which are drawn to the surface by mainstream entrainment react to the temperature of the entrainment flow which is higher than the coolant core. Therefore the temperature of these particles does not drop below the ST value and they mainly deposit on the aft-side of the jet as shown in Figure 3. As a result, with increase in the blowing ratio erosion occurs on the fore-side of the coolant jet, where coolant remains close to the surface.

Figures 7 and 8 show the averaged impact velocity and impact angle for 5 micron particles. At the low blowing ratio, the impact angle is a function of the leading edge curvature and decreases downstream of the coolant hole, indicating direct impacts. As blowing ratio increases, the particles impact the surface at much shallower angles on the fore-side due to the entrainment. In all cases, the impact velocity increases downstream of the coolant hole, due to the accelerated flow.

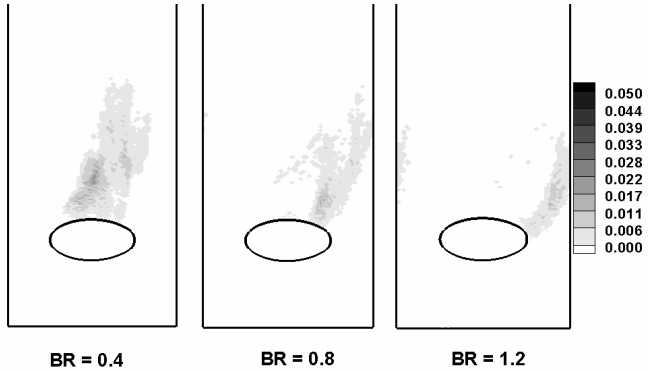

Figure 6. Percentage of 5 micron erosive particle on the surface (out of all 5 micron particles)

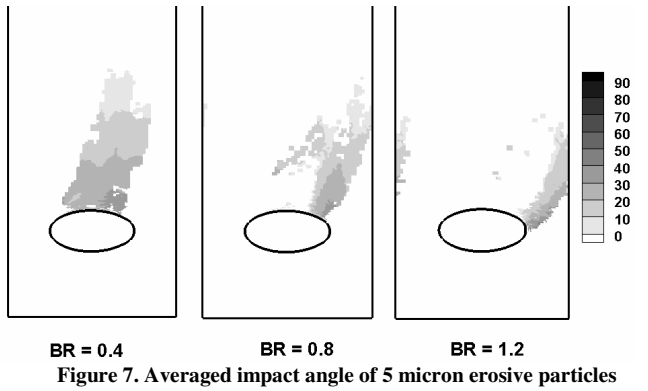

Figure 7. Averaged impact angle of 5 micron erosive particles

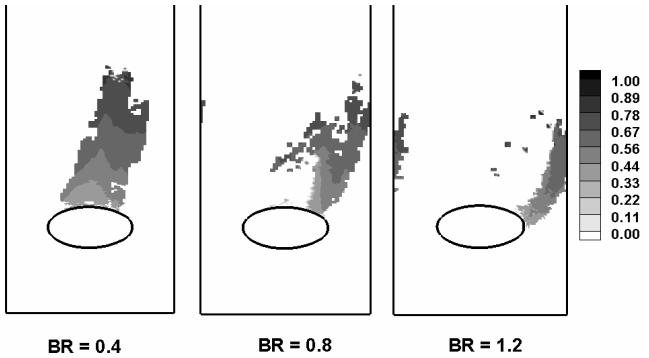

Figure 8. Averaged impact velocity (normalized by u_∞) of 5 micron erosive particles

The 5 micron particles also contribute to the erosive wear inside the coolant hole (Figure 9). These particles, on entry in to the coolant jet, have enough residence time to solidify before impacting on the coolant hole walls. Increase in blowing ratio decreases the number of erosive hits, as it did for the deposited particles. This is due to the stronger momentum of the coolant jet which prevents particles with a small momentum Stokes number to enter the coolant hole. The impact angle at lower blowing ratio is slightly higher on the wall facing the flow due to the almost normal impact of the particles which enter the coolant hole from the upstream edge. Some particles which enter the hole are blown out again and impact the upstream lip of the coolant hole (Figure 10). The impact velocities range from 0.10 to 0.4 (Figure 11).

Figure 9. Percentage of 5 micron erosive particle in the coolant hole (out of all 5 micron particles)

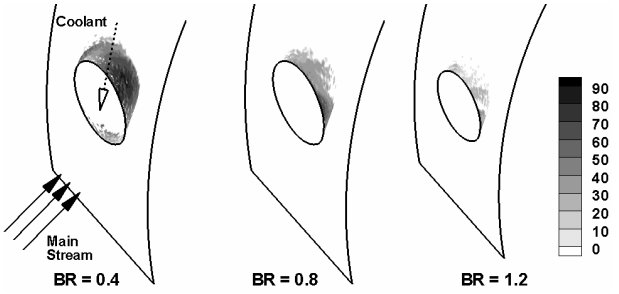

Figure 10. Impact angle of 5 micron erosive particles

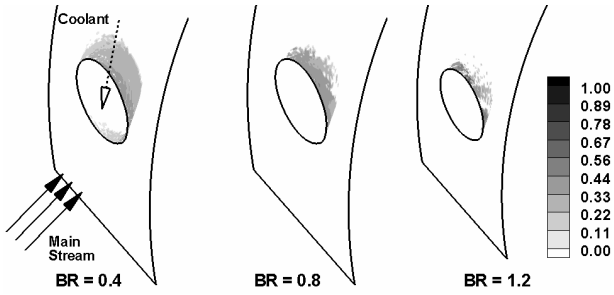

Figure 11. Impact velocity of 5 micron erosive particles

Although the 10 micron particles do not contribute to any erosion on the surface, at BR=1.2, the coolant jet momentum slows a small fraction of 10 micron particles enough to increase their residency time and allowing them to solidify. Due to their large momentum Stokes number, these particles travel further into the coolant hole before they are washed out by the coolant flow. Therefore, unlike the 5 micron particles the effects of these erosive particles are observed at about 1*d* into the coolant hole as shown in Figure 12. The impact angle of these particles is also found to be high due to the circulation of these particles inside the coolant hole.

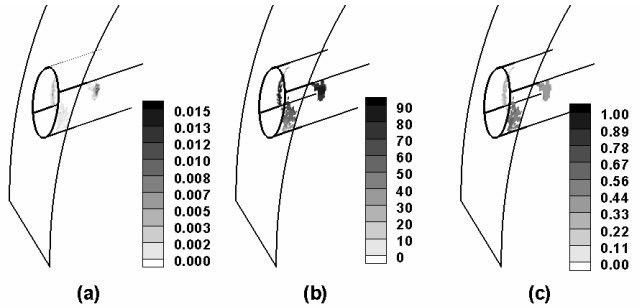

Figure 12. (a) Percentage of 10 micron erosive particle in the coolant hole (out of all 10 micron particles); (b) Impact angle; (c) Impact velocity of at B.R.=1.2

Figure 13 illustrates the overall percentage of erosive 5 and 10 micron particles. As stated before, the percentage of 5 micron erosive particles decrease linearly with an increase in the blowing ratio. Less than one percent of the 10 micron particles become erosive when they enter into the coolant hole.

The Energy Fraction of Erosive Particles (EFEP) is calculated as the kinetic energy of erosive particles that could potentially be transferred to the surface on impact normalized by the incoming kinetic energy of the particles for a given size:

$$(EFEP)_{\mathbf{p}} = \frac{\sum_{surface}\sum_{time} 1/2 m_{erosive} V_{normal}^2}{\sum 1/2 m_{\mathbf{p}} u_\infty^2} \qquad (6)$$

where V_{normal} is the surface normal component of the impact velocity, and m is the mass of particles.

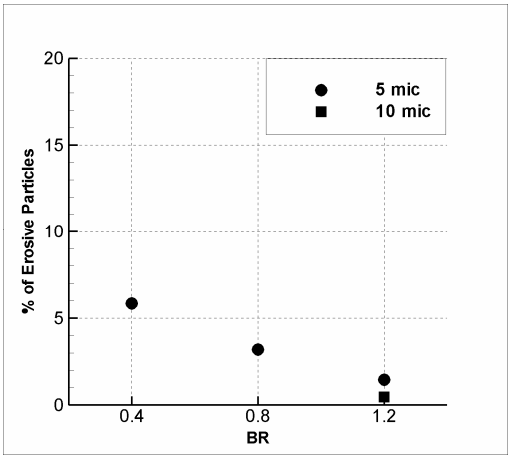

Figure13. Percentage of erosive particles out of total particles of each size

Table 4 summarizes EFEP at each blowing ratio. The potential for erosive wear is higher in the coolant hole than on the surface. On the surface, erosive wear is mostly caused by 5 micron particles, but is an order of magnitude smaller than that inside the coolant hole. Overall, EFEP decreases with an increase in the blowing ratio except at BR=1.2 when 10 micron particles are erosive in the coolant hole.

Table 4. EFEP

B.R.	Particle Size, μm	5	10
0.4	Coolant Hole	2.06E-03	-
	Vane surface	6.02E-04	-
	Total EFEP	2.66E-03	-
0.8	Coolant Hole	1.26E-03	-
	Vane surface	2.35E-04	-
	Total EFEP	1.49E-03	-
1.2	Coolant Hole	3.13E-04	2.15E-04
	Vane surface	1.78E-04	-
	Total EFEP	4.91E-04	2.15E-04

Summary and Conclusions

The paper investigates the deposition and erosion caused by Syngas ash particles in a film cooled leading edge region of a representative turbine vane. The carrier phase is predicted using Large Eddy Simulation and three ash particle sizes of 1, 5, and 10 microns are investigated. A threshold ash softening temperature is assumed to determine the state of particles on impact and hence, distinguish between deposition and erosion.

The 1 micron particles with momentum Stokes number St_p = 0.03 (based on approach velocity and cylinder diameter), follow the flow streamlines around the leading edge and few particles reach the blade surface – only when entrained by the coolant jets. The 10 micron particles, on the other hand with a high Stokes number, St_p = 3, directly impinge on the surface, with blowing ratios (0.4, 0.8 and 1.2) having a minimal effect. The 5 micron particles with St_p=0.8, show the largest receptivity to coolant flow and blowing ratio once the particles penetrate into the region of coolant injection.

More than 90% of the injected 10 micron particles deposit on the surface and in the coolant hole upon impact. 1 micron particles, on the other hand, respond to the entrainment on the aft-side of the coolant jet and their rate of deposition increases with increase of the blowing ratio. The deposition of 5 micron particles, on the other hand decreases with an increase in B.R. On a number basis, about 85-90% of 10 micron particles deposit on the surface with 40-50% of 5 micron particles. Less than 1% of 1 micron particles deposit. Overall there is a slight decrease in percentage of particles deposited with increase in blowing ratio.

Particles which have low thermal inertia or low thermal Stokes numbers cool below the softening temperature and contribute to erosive wear. In this respect, 5 micron particles contribute almost exclusively to erosive wear on the surface and in the coolant hole. While most 1 micron particles are relegated to the outer flow, the larger 10 micron particles with higher thermal inertia result exclusively in deposition on the surface and in the coolant hole. A notable exception is at B.R.=1.2, when 10 micron particles are slowed sufficiently in the coolant hole to allow them to solidify and become erosive. Most of the erosive wear occurs in the coolant hole and is attributed to 5 micron particles, which have lower thermal inertia and solidify faster.

References

[1] Wenglarz, R.D., 1985. "Deposition, erosion and corrosion protection for coal-fired gas turbine". ASME paper No. 85-IGT-61

[2] Krishnan, V., Kapat, J.S., Sohn, Y.H., Desai, V.H., 2003. "Effect of film cooling on low temperature hot corrosion in a coal fired gas turbine". ASME paper No. GT2003-38593

[3] Hamed, A., 1988. "Effect of particle characteristics on trajectories and blade impact patterns". Journal of Fluid Engineering, Vol. 110, pp 33-37

[4] Raubenheimer, D.S.T., 1990. "Selection and operation of gas turbine air filters". Turbomachinery International, Vol. 31, No. 1, Jan/Feb. Issue, pp 26-33

[5] Smialek, J.L., Archer, F.A., Garlick, R.G., 1992. "The chemistry of Saudi Arabian sand: a deposition problem on helicopter turbine airfoils". 3rd International SAMPE Metals and Metals Processing Conference, Society for the

Advancement of Material and Process Engineering, Vol. 3, pp M63-M77
[6] Hamed, A., Tabakoff, W., 1994. “Experimental and Numerical Simulation of Ingested Particles in Gas Turbine Engines". AGARD (NATO) 83rd Symposium of Propulsion and Energetics Panel on Turbines, Rotterdam, Netherlands, 25-28 April 1994.
[7] Metwally, M., Tabakoff, W., Hamed, A., 1995. “Blade erosion in automotive gas turbine engine”. Journal of Engineering for Gas Turbine and Power, Vol.117, pp 213-219
[8] Walsh, W.S., Thole, K.A., Joe, C., 2006. “Effects of sand ingestion on the blockage of film-cooling holes”. ASME paper No. GT2006-90067
[9] Bons, J.P., Crosby, J., Wammack, J.E., Bentley, B.I., Fletcher, T.H., 2005. “High pressure turbine deposition in land based gas turbines from various Synfuels”. ASME paper No. GT2005-68479
[10] Crosby, J., Lewis, S., Bons, J.P., Weiguo, A., Fletcher, T.H., 2007. “Effects of particle size, gas temperature, and metal temperature on high pressure turbine deposition in land based gas turbine from various synfuels”. ASME paper No. GT2007-27531
[11] Sundaram, N., Thole, K.A., 2006. “Effects of surface deposition, hole blockage, and TBC spallation on Vane endwall film-cooling”. ASME paper No. GT2006-90379
[12] Shah, A. and Tafti D. K., 2007. “Transport of Particulates in an Internal Cooling Ribbed Duct”. ASME J. Turbomachinery, 129(4), pp. 816-825.
[13] Rozati, A., Tafti, D.K., 2008. “Large-eddy simulation of leading edge film cooling: Analysis of flow structures, effectiveness, and heat transfer coefficient”. International Journal of Heat and Fluid Flow, Vol. 29, No. 1, pp 1-17
[14] Rozati, A., Tafti, D.K., 2007. “Effect of coolant-mainstream blowing ratio on leading edge film cooling flow and heat transfer”. International Journal of Heat and Fluid Flow, *Accepted for publication*
[15] Seggiani M., Pannocchia G., 2003. “Prediction of coal ash thermal properties using partial least squares regression”. Ind. Eng. Chem. Res., Vol. 42, No. 20, pp 4919-4926
[16] Shah, A., 2005. “Development and application of a dispersed two-phase flow capability in a general multi-block Navier Stokes solver” MS Thesis, Mech. Eng., Virginia Tech
[17] Clift, R., Grace, J.R., and Weber, M.E., 1978. “Bubbles, Drops and Particles”. Academic Press, New York
[18] Incropera, F.P., Dewitt, D.P., Bergman, T.L., Lavine, A.S., 2007. “Fundamentals of heat and mass transfer”. Wiley, 6th edition, pp 434